



OPEN

SUBJECT AREAS:
GENETIC INTERACTION
CELL GROWTH
CANCER GENETICS
CANCER MODELSReceived
11 June 2013Accepted
7 January 2014Published
11 February 2014Correspondence and
requests for materials
should be addressed to
M.A.J. (mjuenger@
ethz.ch)

Src tyrosine kinase signaling antagonizes nuclear localization of FOXO and inhibits its transcription factor activity

Margret H. Bülow^{1,3}, Torsten R. Bülow², Michael Hoch³, Michael J. Pankratz² & Martin A. Jünger¹

¹Institute of Molecular Systems Biology, Swiss Federal Institute of Technology (ETH) Zurich, 8093 Zurich, Switzerland, ²Life and Medical Sciences (LIMES) Institute, Department of Molecular Brain Physiology and Behavior, University of Bonn, 53115 Bonn, Germany, ³Life and Medical Sciences (LIMES) Institute, Program Unit Development and Genetics, Laboratory for Molecular Developmental Biology, University of Bonn, 53115 Bonn, Germany.

Biochemical experiments in mammalian cells have linked Src family kinase activity to the insulin signaling pathway. To explore the physiological link between Src and a central insulin pathway effector, we investigated the effect of different Src signaling levels on the *Drosophila* transcription factor dFOXO *in vivo*. Ectopic activation of Src42A in the starved larval fatbody was sufficient to drive dFOXO out of the nucleus. When Src signaling levels were lowered by means of loss-of-function mutations or pharmacological inhibition, dFOXO localization was shifted to the nucleus in growing animals, and transcription of the dFOXO target genes *d4E-BP* and *dInR* was induced. dFOXO loss-of-function mutations rescued the induction of dFOXO target gene expression and the body size reduction of Src42A mutant larvae, establishing dFOXO as a critical downstream effector of Src signaling. Furthermore, we provide evidence that the regulation of FOXO transcription factors by Src is evolutionarily conserved in mammalian cells.

Intracellular signaling cascades that elicit physiological responses triggered by extracellular stimuli such as hormones or nutrients mainly rely on the reversible phosphorylation of proteins¹, regulating their enzymatic activity, conformation, subcellular localization, stability or interaction with other proteins. The interplay between protein kinases and protein phosphatases orchestrates the activity profile of the cellular proteome and therefore plays a central role in the regulation of most biological processes. Genetic alterations or environmental influences that lead to the dysregulation of protein kinases or phosphatases can lead to diseases such as cancer, diabetes and inflammatory disorders. In the case of cancer, the impact of protein phosphorylation on the malignant transformation of cells has been recognized decades ago, when it was discovered that several animal tumor viruses encode protein tyrosine kinases¹. The first known protein tyrosine kinase, c-Src, was identified as the cellular progenitor of the viral kinase v-Src, which is the transforming protein of the oncogenic Rous sarcoma virus (RSV)². Another intracellular driver of growth and ultimately transformation is the insulin signaling pathway. Several publications reported that in mammalian cells, c-Src is required for the transduction of signaling from the insulin or insulin-like growth factor (IGF) receptor to downstream effectors^{3–7}. Most of these studies suggest that Src function is required in the upstream part of the signaling pathway - in some contexts, Src associates with and/or is activated by the ligand-bound receptor^{8–12}. Intersections of Src signaling with the insulin/IGF pathway have also been described at the level of insulin receptor substrate (IRS) proteins^{13,14}, phosphoinositide 3-kinase (PI3K)¹⁵ and in the activation of AKT^{16–19}. The main limitation of these biochemical studies is that they are mostly based on experiments in cell culture and often employ tools like the rather unspecific Src inhibitors PP1 and PP2, and therefore it is difficult to deduce the relevance of Src signaling in actual *in vivo* conditions in the living organism from them. To fill this knowledge gap, genetic analyses in model organisms such as *Drosophila* are well suited. In the fruit fly, a link between Src family kinase (SFK) signaling and insulin signaling has not been established. However, it was discovered in the large-scale yeast two-hybrid interactome study by Giot et al. that both fly Src family kinases, Src42A and Src64B, interact physically with the adapter protein DOK (Downstream of kinase) which contains a pleckstrin homology (PH) domain and a phosphotyrosine-binding (PTB) domain like CHICO and its mammalian IRS orthologs²⁰. This binding might provide a way



by which Src kinases could be recruited into insulin-dependent signaling complexes. In agreement with this hypothesis, the recently identified adapter protein IRS5/DOK4 binds to SFKs upon phosphorylation by the insulin receptor²¹. The goal of the work presented here was to evaluate a possible role of SFKs in insulin signaling in a physiological *in vivo* setting, and to characterize this impact on the pathway by focusing on a signaling component that has so far not been characterized to be regulated by Src. We investigated the effect of altered Src signaling levels on the transcription factor dFOXO, a central downstream transcriptional mediator of the cellular response to insulin-like peptides in the fly^{22–24}, which is also conserved in higher organisms.

Results

Activation of Src42A prevents starvation-induced nuclear accumulation of dFOXO. Subcellular localization of dFOXO can be used as a readout for insulin signaling activity. In cultured cells, stimulation with insulin leads to nuclear exclusion, and serum deprivation to nuclear accumulation of dFOXO. During the larval stages of *Drosophila* development, dFOXO is not completely excluded from the nucleus under fed conditions, but rather equally distributed between nucleus and cytoplasm in the fatbody cells of growing 2nd and early 3rd instar larvae. During the 3rd larval instar, dFOXO localization in the fatbody shifts more towards nuclear, even when larvae are still feeding (not shown). We therefore performed all the experiments investigating dFOXO localization with 2nd or early 3rd instar larvae. The hs-FLP/FRT system²⁵ was used to generate GFP-marked transgene overexpression clones within a control tissue composed of wild type cells. As a positive control, we tested whether in starved animals, nuclear accumulation of dFOXO can be blocked by overexpressing the insulin receptor dInR in clones of cells. Under these conditions, dFOXO was nuclear in wildtype fatbody cells, whereas the cells overexpressing the insulin receptor (marked with GFP in supplementary figure 1A and 1C) showed a dramatic overgrowth phenotype as well as a loss of the nuclear dFOXO signal (supplementary figure 1B). Figure 1 displays the effect of clonal overexpression of wild-type and constitutively active (“CA”) alleles of Src42A and Src64B on nuclear dFOXO localization and cell size under starvation conditions. The activated Src alleles Src42A[Y511F] and Src64B[Y547F] carry tyrosine to phenylalanine mutations which ablate the inactivating conserved phosphorylation site modified by the negative upstream regulator C-terminal Src kinase (CSK). The only statistically significant effect on dFOXO localization was observed upon expression of Src42-CA, which inhibited nuclear dFOXO accumulation and had a positive effect on cell size (Figure 1A–D). The wild type allele of Src42A did not confer the same effects upon overexpression, neither on cell size nor on dFOXO localization (Figure 1E–G). Constitutively active Src64B-CA had a positive effect on cell size, but no effect on nuclear dFOXO (Figure 1I–L), while expression of wild-type Src64B had no significant effect on cell size, and only a mild one on dFOXO localization (Figure 1M–P). To rule out the possibility that the different effects of the Src alleles on cell size and dFOXO localization are a consequence of transgene expression levels rather than kinase activity or specificity, we expressed the four Src transgenes used in this study with a fatbody-specific driver line (cg-Gal4)²⁶ and an eye-specific driver (GMR-Gal4)²⁷ and measured Src42A and Src64B transcript levels by quantitative realtime PCR in total larval and adult head extracts, respectively. We detected no significant differences in expression level between the transgenic lines (data not shown), arguing that the effect of Src42A-CA is specific to the constitutive activation of Src kinase and not caused by variations in expression levels. In addition, we assessed whether inhibition of Src signaling by overexpression of the negative upstream regulator CSK has an effect on cell size or dFOXO localization, as it may be expected that under fed conditions,

lowering of Src activity by CSK leads to reduced cell size and nuclear dFOXO accumulation. However, overexpression of the CSK did not have an effect on cell size or dFOXO localization in the fatbody of starved or yeast-fed larvae (supplementary figure 1D–I).

Reduction of Src42A function leads to nuclear translocation and activation of dFOXO. We next asked whether a reduction in Src42A signaling levels would affect the localization and activity of dFOXO. To address this issue, we used two characterized loss-of-function alleles of Src42A. *Src42A*^{k10108} and *Src42A*^{lp45} are both P-element insertions in the 5' untranslated region (UTR) of the *Src42A* gene. In both cases, homozygous larval lethality is rescued by mobilization of the P-elements as well as expression of *Src42A* transgenes^{28,29}. We analyzed the subcellular localization of dFOXO in these *Src42A* mutant lines under well fed conditions (yeast) in the fatbodies of 2nd instar larvae. In wildtype animals, dFOXO is distributed between nucleus and cytoplasm (Figure 2A). In heterozygous Src mutants (*Src42A*^{k10108/+}), we observed a phenotypic range from a subcellular distribution similar to the one observed in wildtype animals (Figure 2B) to a distinct nuclear localization (Figure 2C). In homozygous *Src42A*^{k10108} larvae, dFOXO was found to be nuclear in all samples examined (Figure 2D). These observations indicate that cytoplasmic localization of dFOXO in fed, growing animals is dependent on intact Src42A signaling. In an attempt to corroborate these findings with a molecular and quantitative readout for dFOXO's activity as a transcription factor, we measured the mRNA abundance of two established dFOXO target genes, *d4E-BP* and *dInR*, in *Src42A* mutant larvae. Both *d4E-BP* and *dInR* expression was strongly induced in both *Src42A* (Figure 2E) and *Src64B* mutants (Figure 2F). *Src42A* mutations elicited a stronger induction than *Src64B* mutations, and in both cases the target gene induction was suppressed by heterozygous dFOXO mutations. This indicates that Src is not only required for the prevention of aberrant nuclear accumulation of dFOXO during periods of organismal growth, but also for the concomitant shutdown of dFOXO target gene expression.

dFOXO mutations suppress Src loss-of-function phenotypes. Homozygous *Src42A*^{lp45} animals mostly die as larvae and the appearance of a few adult escapers has been reported when reared at 18°C (ref. 29). Under our laboratory conditions and at 25°C, the homozygous *Src42A*^{lp45} mutation lead to 100% larval lethality during the 3rd instar. To assess whether dFOXO is a physiologically relevant downstream effector of Src42A, we generated double mutant animals for *Src42A* and *dFOXO* and analyzed the effect of lowering *dFOXO* gene dosage on the *Src42A* phenotype. We observed a strong genetic interaction between *Src42A* and *dFOXO*. Not only was the elevated *d4E-BP* and *dInR* expression in heterozygous *Src42A* mutant animals restored to near-wildtype levels, but also the larval size reduction of homozygous *Src42A*^{lp45} animals was dominantly suppressed by the presence of one copy of the *dFOXO*²⁵ allele²² in age-matched animals (Figure 2G and H). Furthermore, the larval lethality of homozygous *Src42A* mutants was rescued to the pupal stage by a heteroallelic combination of *dFOXO*²¹ and *dFOXO*²⁵ (*dFOXO* alleles which as homozygous single mutants only display significant phenotypes under conditions of reduced insulin signaling, starvation or oxidative stress) (Figure 2I). This epistasis of *dFOXO* over *Src42A* demonstrates that under physiological conditions *in vivo*, dFOXO is a critical downstream component of *Drosophila* Src signaling. To exclude the possibility that the phenotypes observed in Src and dFOXO mutants were due to abnormal feeding behavior, we used colored yeast paste to confirm that both Src and dFOXO mutant larvae feed normally (Supplementary Figure 2).

Pharmacological inhibition of Src elicits dFOXO-dependent transcriptional phenotypes. To complement our genetic experiments, we performed larval feeding of SU6656, a specific inhibitor of SFKs³⁰,

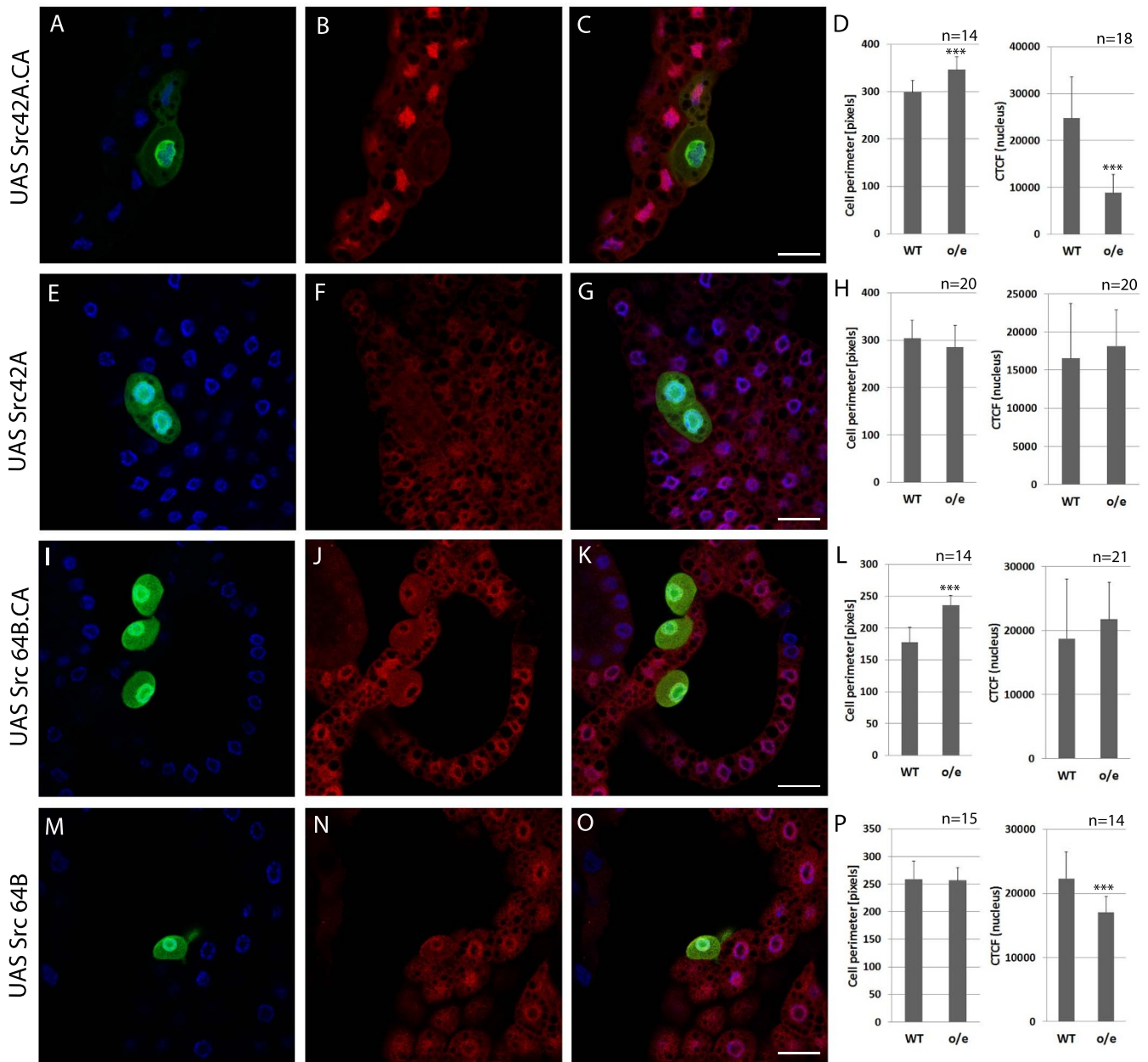


Figure 1 | Overexpression of constitutively active Src42A inhibits nuclear accumulation of dFOXO under conditions of starvation. Fatbody clones from early 3rd instar larvae are shown. Larvae were raised on yeast for 48 h and starved on PBS for 24 h. Immunostainings were performed with mouse α -GFP (green), rabbit α -dFOXO (red). The nuclear DAPI counterstain is shown in blue. (A–C) Wildtype cells show nuclear dFOXO while nuclear shuttling is blocked in cells expressing constitutively active Src42A. These cells are larger than wildtype cells, thus, they display no starvation-induced growth arrest. Genotype is *y w hs-flp; Act > CD2 > Gal4 UAS-GFP/UAS Src42A.CA*. (D) Graphs show the perimeter of wildtype cells (WT) compared to cells expressing Src42A.CA (o/e) and the corrected total cell fluorescence (CTCF) calculated only for the nuclear region as a quantification of nuclear dFOXO abundance. Cells expressing constitutively active Src42A are significantly larger and have lower nuclear dFOXO levels than wildtype cells. (E–G) No significant differences in cell size or nuclear dFOXO are observed in Src42A.WT expressing cells. Genotype is *y w hs-flp; Act > CD2 > Gal4 UAS-GFP/UAS Src42A.WT*. (H) Measuring the cell perimeter and calculating the nuclear fluorescence intensity shows that cells overexpressing wildtype Src42A are not significantly larger than wildtype cells and have similar nuclear dFOXO levels. (I–K) GFP-positive cells are slightly larger than wildtype cells and display nuclear dFOXO levels that are not significantly altered in comparison to wild-type cells. Genotype is *y w hs-flp; Act > CD2 > Gal4 UAS-GFP/UAS Src64B.CA*. (L) Cells expressing constitutively active Src64B are significantly larger than wildtype cells but do not show a significant reduction of nuclear dFOXO signal. (M–O) Cells overexpressing the wildtype form of Src64B are of similar size like the surrounding cells and show slightly reduced starvation-induced nuclear shuttling of dFOXO. Genotype is *y w hs-flp; Act > CD2 > Gal4 UAS-GFP/UAS-Src64B.WT*. (P) The graphs show that overexpression of a wildtype form of Src64B has no effect on cell perimeter, and a slight but significant one on nuclear fluorescence derived from the dFOXO antibody in fatbody cells. Scale bars represent 20 μ m. Statistical significance was tested using an unpaired, two-tailed Student's t-test. Asterisks represent * = $p < 0.05$, ** = $p < 0.01$, *** = $p < 0.001$.

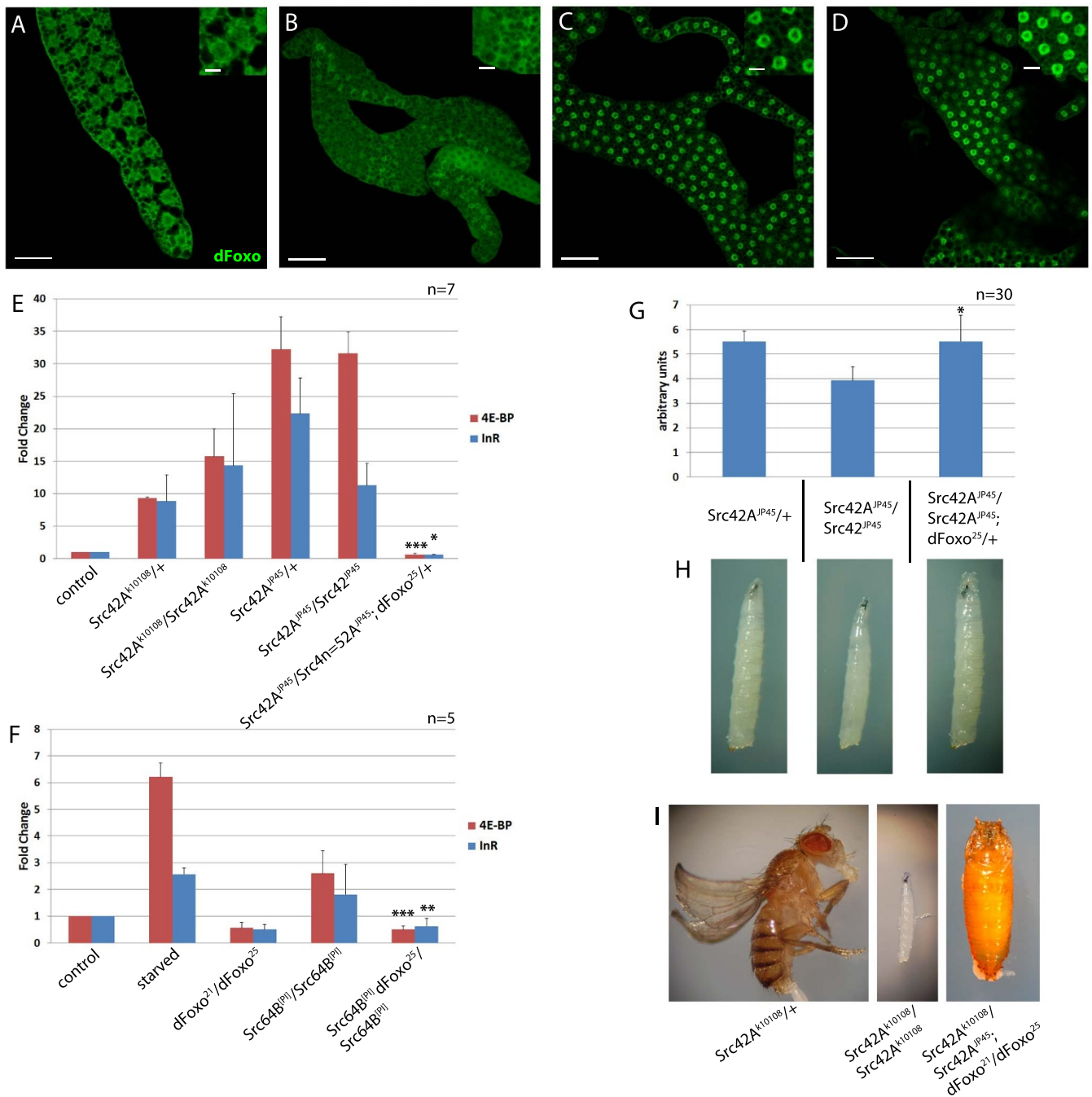


Figure 2 | Loss of Src kinase function leads to dFOXO nuclear translocation, target gene activation and dFOXO-dependent growth inhibition. (A–D) Confocal sections of fatbodies of 2nd instar larvae, fed on yeast, are shown. Tissues were stained using an antibody against dFOXO. Insets show close-ups of selected cells. dFoxo is cytoplasmic in fatbody cells of fed wildtype larvae and shuttles to the nucleus in *Src42A* mutants. Genotypes are: wildtype (A), *w; Src42A^{k10108}/CyO* (B, C) and *w; Src42A^{k10108}/Src42A^{k10108}* (D). (E, F) Real-time qPCR analyses measuring the expression of the dFOXO target genes *d4E-BP* and *dlnR* in larval extracts are shown. Target gene expression is increased in the heterozygous and homozygous *Src42A* mutants *Src42A^{k10108}* and *Src42A^{IP45}* in well fed larvae. This effect is suppressed in homozygous mutants by one copy of the *dFOXO²⁵* loss-of-function allele. Upregulation of *d4E-BP* and *dlnR* as well as the dFOXO-dependence of this effect are also observed in *Src64B* mutants (F). Genotypes are *w; Src42A^{k10108}/CyO-GFP*, *w; Src42A^{k10108}/Src42A^{k10108}*, *w; Src42A^{IP45}/CyO-GFP*, *w; Src42A^{IP45}/Src42A^{IP45}*, *w; Sp/CyO*, *dFOXO²¹/dFOXO²⁵*, *w; Src64B^[PI]/Src64B^[PI]* and *w; Src64B^[PI]/dFOXO²⁵/Src64B^[PI]*. (G, H) Growth is impaired in 3rd instar larvae which are homozygous for *Src42A^{IP45}*. This effect is rescued by heterozygosity for *dFOXO²⁵*, demonstrating that the size reduction is dFOXO-dependent. (I) Flies heterozygous for a *Src42A* mutation are fertile and viable, whereas homozygous mutants display larval lethality. Transheterozygous mutants with two *Src42A* alleles are partially rescued by the heteroallelic combination *dFOXO²¹/dFOXO²⁵* and reach the pupal stage. Statistical significance was tested using unpaired, 2-tailed Student's t-test. Asterisks represent * = $p < 0.05$, ** = $p < 0.01$, *** = $p < 0.001$. Significance was tested against the corresponding value of the homozygous *Src* mutant without *dFOXO* mutations. Scale bars represent 50 μ m in main pictures and 20 μ m in insets.



to inhibit Src signaling *in vivo*. Quantitative realtime PCR was employed to quantify expression changes of Src genes and dFOXO target genes. Our first finding from this set of experiments was that both pharmacological and genetic inhibition of Src reduced mRNA expression levels of both *Src42A* (Figure 3A) and *Src64B* (Figure 3B). This suggests the existence of some kind of feedback mechanism, in which Src kinases regulate their own expression. Evidence that this feedback mechanism probably involves dFOXO is presented in Supplementary Figure 3. This finding also illustrates that it is difficult to separate the effects of the two SFKs solely by genetic means using loss-of-function mutations. Figure 3C shows the effect of pharmacological Src inhibition on the expression levels of the dFOXO target genes *d4E-BP* and *dInR*. SU6656 feeding strongly induced the expression of both genes (Figure 3C, bar pairs 1–3), with a more pronounced effect on *d4E-BP*, suggesting an activation of dFOXO. Indeed the observed target gene induction is dependent on dFOXO function, as it is completely suppressed in the presence of heterozygous *dFOXO* mutations (Figure 3C, bar pairs 4–9). Also the localization of dFOXO is shifted towards a stronger nuclear

abundance by inhibitor feeding (Figure 3E) in comparison to the negative control treatment (Figure 3D). Based on a quantification of dFOXO signal in the nucleus, this effect is statistically significant (Figure 3F). These observations are in agreement with our genetic experiments that establish dFOXO as a mediator of Src loss-of-function phenotypes.

Growth stimulation by the insulin receptor is partially dependent on Src activity.

To assess the possibility that Src kinases are mediators of the insulin pathway in *Drosophila*, we addressed the question whether insulin-dependent cell growth would be modulated by alterations in Src signaling. We therefore overexpressed the insulin receptor in fatbody cell clones of animals that were starved on PBS (Figure 4). Under these conditions, InR expression leads to a dramatic cellular overgrowth and nuclear exclusion of dFOXO (Figure 4A–C). Feeding the starved larvae with 0.5 mM (Figure 4D–E) or 1 mM (Figure 4G–I) of the Src inhibitor SU6656 leads to a significant reduction of the size of the InR-expressing cells, without influencing the nuclear exclusion of dFOXO. Quantitative analysis of

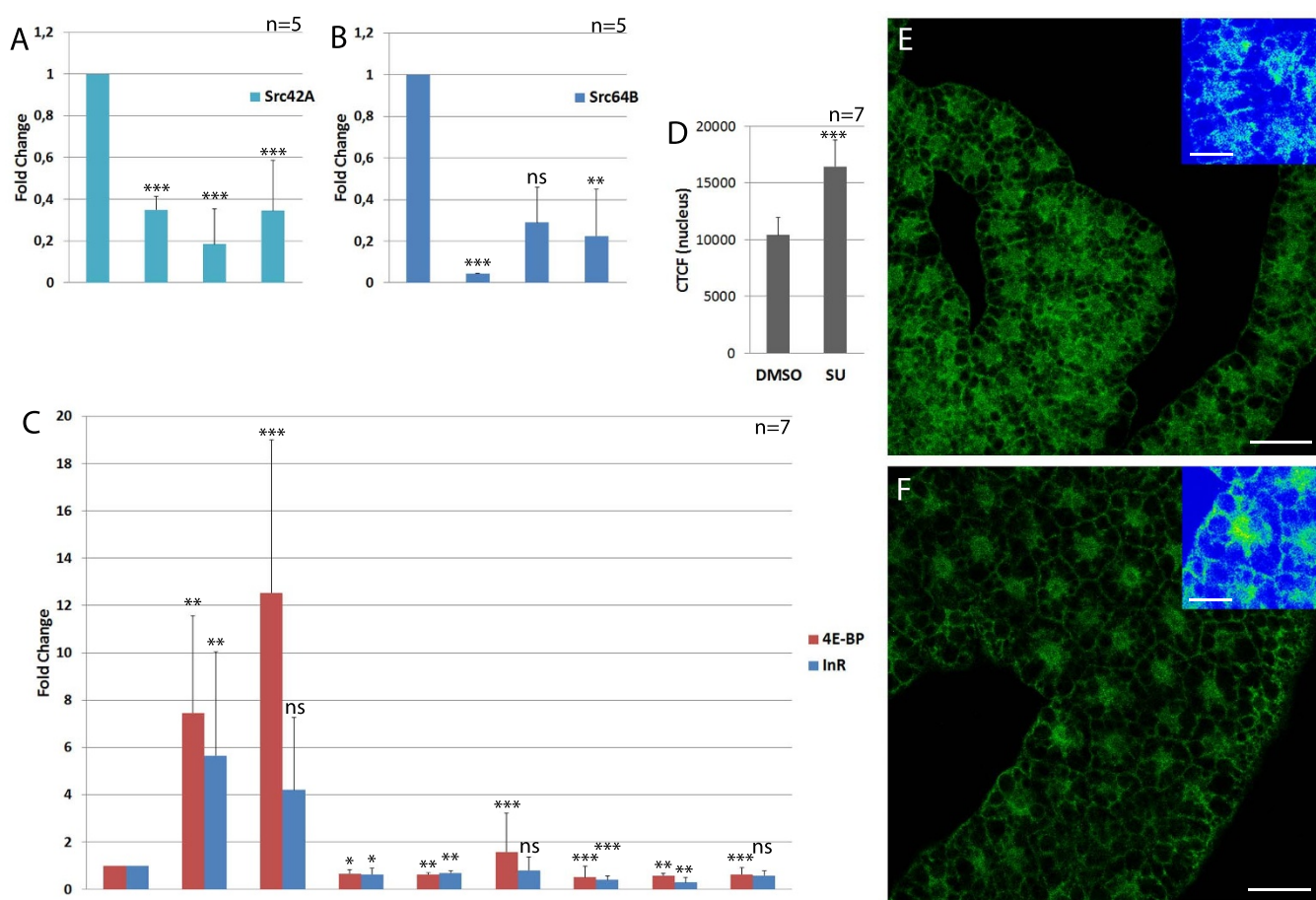


Figure 3 | Pharmacological inhibition of *in vivo* SFK signaling elicits reduced Src expression and induction of dFOXO-dependent transcription. (A, B) Quantitative real-time PCR from total RNA extracts from 2nd instar larvae are shown. *Src42A* expression levels are reduced in *Src64B* mutants and *vice versa*. (C) Quantitative real-time PCR from total RNA extracts from larvae are shown. Animals were fed on yeast for 48 h and treated with the Src inhibitor SU6656 for 24 h. **Bar pairs 1–3:** wildtype treated with DMSO as a control or 0.5 mM or 1 mM of SU6656, respectively. SU6656 treatment strongly upregulates the expression of 4E-BP in a dose-dependent manner. **Bar pairs 4–6:** Heterozygous *dFOXO²¹* mutants were treated with DMSO or Src inhibitor. Only high concentrations of SU6656 show a weak and non-significant effect on 4E-BP expression. **Bar pairs 7–9:** Heterozygous *dFOXO²⁵* mutants were treated with DMSO or Src inhibitor. SU6656 has no significant effect on 4E-BP expression levels. (D, E) Fatbody tissue from early 3rd instar wildtypic larvae treated with DMSO (D) or 1 mM SU6656 (E) immunostained with a dFOXO antibody. Insets show fluorescence intensity. The inset false colors correspond to increasing fluorescence intensity in the order blue-green-yellow-red (weak to strong). dFOXO translocates to the nucleus in fatbody cells from SU6656-treated animals. (F) Quantification of the nuclear dFOXO levels using the CTCF value. Cells from animals treated with SU6656 show a significantly stronger nuclear dFOXO signal compared to controls. Statistical significance was tested using ANOVA with Tukey-Kramer post test, except for (B) where data was analyzed with a Kruskal-Wallis test and Dunn post test. Asterisks represent * = $p < 0.05$, ** = $p < 0.01$, *** = $p < 0.001$, or ns for non-significant differences. Significance was tested against the respective wild type control.



cell size (Figure 4J) shows that the effect of the Src inhibitor on the size of InR-expressing cells is highly significant. We conclude from this finding that active Src is needed to promote the growth-inducing signaling events triggered by activation of the insulin receptor. The dependence of the InR-dependent signaling of Src seems to be a partial one, because Src inhibition does not reduce the size of InR-expressing cells to wildtype cell dimensions.

Inhibition of SFK signaling in mouse cells leads to nuclear accumulation of FOXO3. The interaction between Src and FOXO in the

model organism *Drosophila* raises the question whether this is conserved in higher organisms. We therefore monitored nucleocytoplasmic shuttling of a mCherry-FOXO3 fusion protein in mouse NIH-3T3 preadipocytes. FOXO3 is one of the three human FOXO transcription factors which are inactivated by insulin/IGF signaling via phosphorylation-dependent cytoplasmic sequestration³¹. In NIH-3T3 cells growing in the serum-containing medium, mCherry-FOXO3 was completely excluded from the nucleus (Figure 5A). Inhibition of PI3K activity with LY294002 lead to a shuttling of mCherry-FOXO3 to the nucleus in the presence of

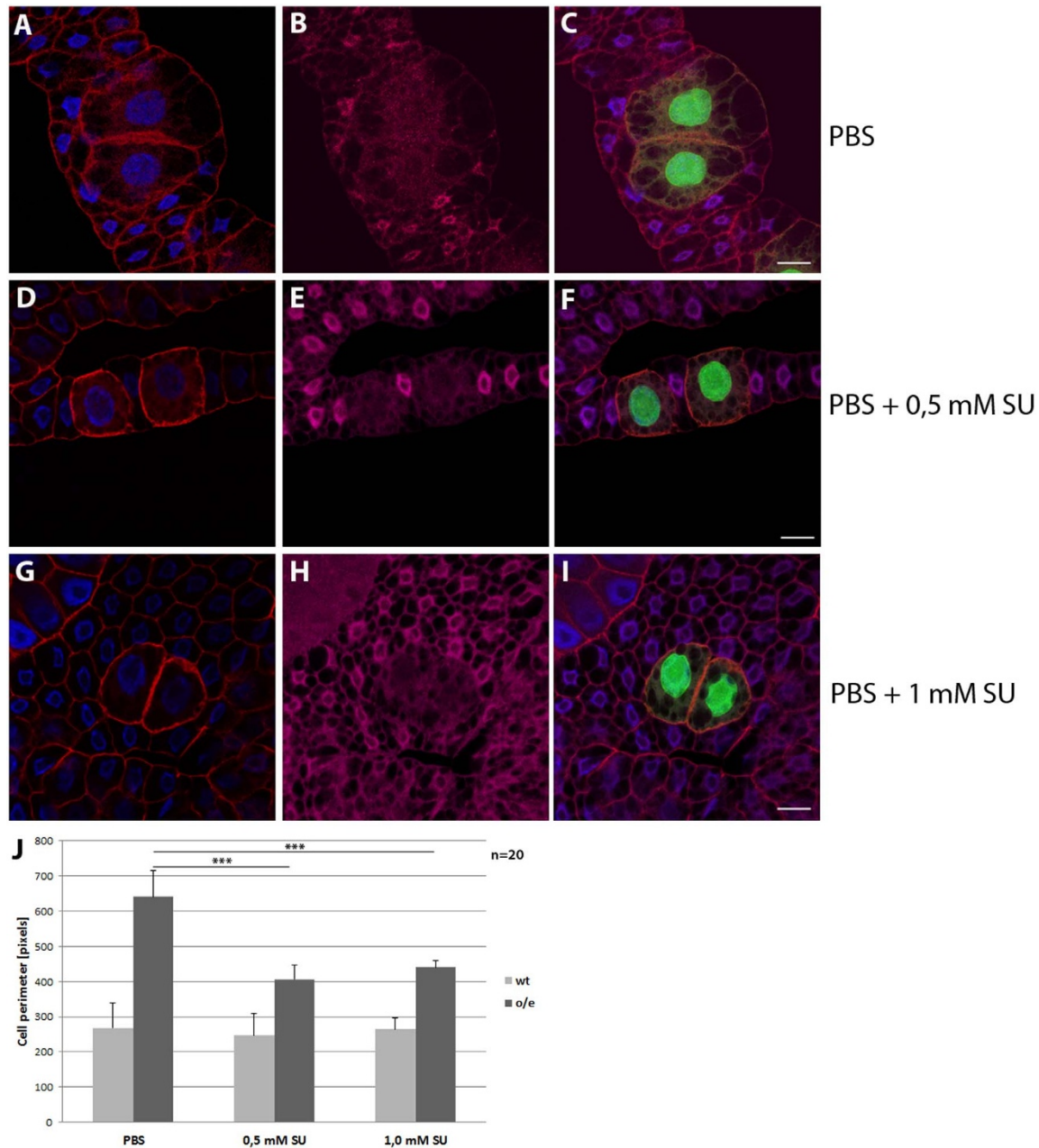


Figure 4 | Insulin receptor-dependent growth stimulation depends on Src activity in the fatbody. Fatbody clones from 3rd instar larvae are shown. Larvae were raised on yeast for 60 h and starved on PBS +/– SU6656 for 16 h. Clones are marked with GFP (green). Immunostaining with mouse α -spectrin (red), rabbit α -dFOXO (magenta) and DAPI (blue). Genotype *y w hs-flp; Act > CD2 > Gal4 UAS-GFP/UAS dInR*. (A–C) Clones overexpressing the insulin receptor from larvae starved on PBS for 16 h. Insulin receptor overexpression induces growth and inhibits dFoxo nuclear shuttling, while the wildtype cells display nuclear dFOXO and subsequent growth arrest. (D–F) When 0.5 mM of the Src-Inhibitor SU6656 is added, the overgrowth of InR overexpression clones in starved tissue is significantly reduced, but dFOXO nuclear exclusion is unchanged. (G–I): Addition of 1 mM SU6656 also reduces overgrowth of InR clones without leading to nuclear dFOXO accumulation. (J) Quantitative analysis of the fatbody clones shows a significant reduction of the overexpression clones upon SU6656 feeding. Error bars represent standard deviation. Scale bars are 20 μ M. Significance was tested using one-way ANOVA with post-tests. Asterisks represent *** = $p < 0.001$.

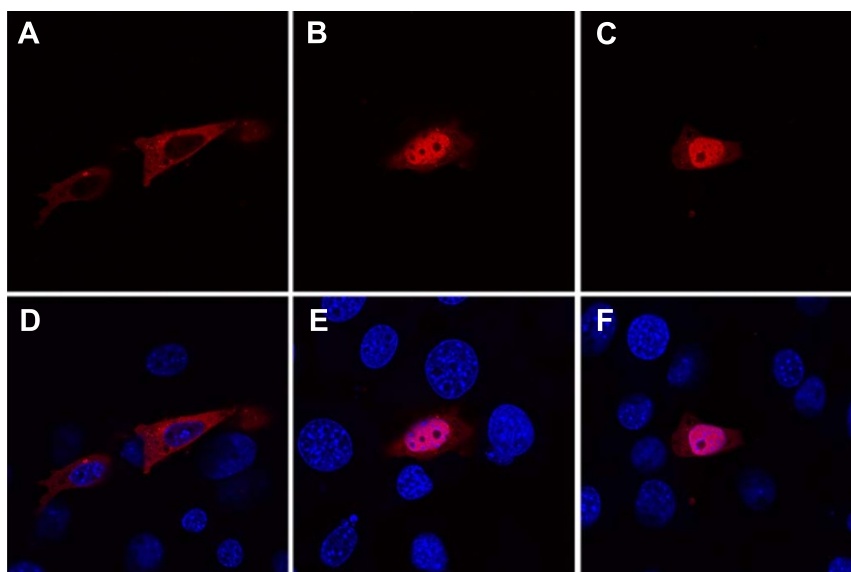


Figure 5 | SFK signaling regulates FOXO localization in mammalian cells. (A, D) In transiently transfected NIH-3T3 mouse fibroblasts, mCherry-FOXO3 is cytoplasmic when cells are growing in FCS-containing medium. (B, E) Under these conditions of serum-dependent growth, inhibition of Src by treatment with 5 μ M SU6656 for 1 h leads to nuclear accumulation of mCherry-FOXO3, as does inhibition of PI3K activity by incubation with 50 μ M of the inhibitor LY294002 for the same time (C, F). Each confocal section displaying the dFOXO antibody signal in red is shown once without (A, B, C) and once with (D, E, F) the blue nuclear DAPI counterstain. The subcellular distributions shown are representative and were observed in all expressing cells examined ($n > 50$ for each condition).

serum (Figure 5C). The same effect was obtained using SU6656. SFK inhibition with SU6656 resulted in nuclear localization of mCherry-FOXO3 in the presence of serum (Figure 5B). We conclude from this observation that the regulation of O subclass forkhead box transcription factors is most likely conserved between species such as fly and mouse.

Discussion

In this study we established a functional genetic interaction between Src kinases and the FOXO transcription factor in *Drosophila* and mammalian cells. The basis for this study was the described implication of Src in the upstream part of the insulin pathway in mammalian cells, between the receptor and AKT. It should be considered that most of the studies linking mammalian Src kinases to the insulin pathway are performed in cultured cells and make use of pharmacological inhibitors of Src family kinases. Special caution should be advised when interpreting conclusions drawn from experiments with the widely used inhibitors PP1 and PP2, because in addition to SFKs they also block platelet-derived growth factor receptor (PDGFR) tyrosine kinase activity with equal potency³⁰. Despite the accumulated biochemical data, solid functional evidence for a requirement of Src activity for insulin signaling in a physiological context is still scarce. We sought to answer this question by manipulating Src signaling levels *in vivo* by genetic and pharmacological means, and using the localization and activity of dFOXO as a readout for insulin pathway activity. Our results show that Src kinases are indeed required for the negative regulation of dFOXO. While artificial activation of Src42A and, to a lesser extent, Src64B prevented the starvation-induced nuclear translocation of dFOXO in the larval fatbody, reduced Src signaling levels lead to nuclear accumulation of dFOXO under high nutrient conditions under which the protein normally displays prominent cytoplasmic localization. In addition to its subcellular localization, also dFOXO transcription factor activity was found to be regulated by Src42A levels. Transcription of the two target genes *dInR* and *d4E-BP* was strongly increased in Src42A mutant animals, which displayed also a body size reduction in the larval stage, and to a lesser extent in Src64B mutants. The presence of a single copy of a dFOXO null mutation was sufficient to reduce the

elevated *dInR* and *d4E-BP* transcription in Src mutant or inhibitor-fed larvae back to wildtype levels. The dFOXO mutation also dominantly rescued the larval size reduction elicited by the lack of Src42A, establishing dFOXO as a critical mediator of Src signaling in the fly. Src seems to act in the insulin pathway between the insulin receptor and dFOXO, as the growth induction by the insulin receptor was demonstrated to partially depend on Src in our experiments. Furthermore, our finding that inhibition of SFK signaling in mouse cells impacted on FOXO localization as well suggests that this interaction has been conserved throughout evolution. The question whether Src42A signals to dFOXO indirectly through upstream components in the insulin pathway or through other upstream kinases, possibly even in a direct manner or in a combination of both, is at this point still open and remains to be investigated.

Methods

Genetics, fly strains, antibodies and constructs. Flies were kept on standard food containing 80 g agar, 1 l molasses, 165 g brewer's yeast, 815 g cornmeal, and 200 ml nipagin (200 g/l 1 ethanol) per 13.3 l of water (see Buch et al.³²) at 25°C. *OregonR-S* (Bloomington stock nr. 4269) flies were used as a wildtype reference. We used the double-balancer line *yw; Sp/CyO-GFP; Tm2 Ubx/Tm6B tb-GFP* to generate *Src42A^{k10108}/CyO-GFP* and *yw; Src42A^{IP45}/CyO-GFP* lines to easily identify homozygous larvae, and to generate transheterozygous lines carrying both *Src42A* and *dFOXO* mutant alleles. To test the transheterozygous lines for presence of both *Src42A* P-element insertions, we performed single fly PCRs using the following primers:

```
Src42A_genomic_fwd: GAGTTAAATGTGAATACGGATGCCAGCCCC
Src42A_genomic_rev: TTGTTTCGCGAATAAGCCGTGCGTGTGAACG
P{LacW} 5': TACGTTAAGTGGATGTCTCTTGCCGACGGG
P{LacW} 3': GGTAAGCTTCGGCTATCGACGGGACC
```

We crossed the heat-shock-inducible Flp/FRT line *hs-flp; Act5C > CD2 > Gal4 UAS GFP/Tm6B* (reference 25) to the Src overexpression lines *w; UAS-Src42A-CA* (Bloomington stock nr. 6410, reference 29), *w; UAS-Src42A* (reference 33), *w; UAS-Src64B-CA* (reference 33) or *w; UAS-Src64B* (Bloomington stock nr. 8477, reference 34) to generate GFP-marked overexpression clones. As a positive control to elicit dFOXO nuclear exclusion, we used a *w; UAS-dInR* line³⁵ to overexpress the insulin receptor. For loss-of-function experiments, we used the *Src42A* mutant alleles *yw; Src42A^{k10108}/CyO* (Bloomington stock nr. 10969, reference 28) and *yw; Src42A^{IP45}/CyO* (reference 29), the *Src64B* mutant allele *yw; Src64B^{PLD1}/Src64B^{IP1J}* (Bloomington stock nr. 7379, reference 36) and the dFOXO mutant alleles *dFOXO²¹* and *dFOXO²⁵* (reference 22) for rescue experiments. The double-balancer line *yw; Sp/CyO-GFP; Tm2 Ubx/Tm6B tb-GFP* was used to generate *Src42A^{k10108}/CyO-GFP* and *yw; Src42A^{IP45}/CyO-GFP* lines to easily identify homozygous mutant larvae based on absence of GFP



fluorescence, and to generate transheterozygous lines carrying both *Src42A* and *dFOXO* mutant alleles. For immunostainings, we used the following primary antibodies: α -FOXO (N-terminus) from rabbit, α -FOXO (C-terminus) from rabbit²⁴ and a monoclonal α -GFP from mouse (Sigma-Aldrich, #G6539). The pcDNA3.1-mCherry-FOXO3 construct encoding a human FOXO3 protein with the red fluorescent mCherry protein fused to its N-terminus, the mCherry coding sequence was amplified from the pRSET_B-mCherry vector³⁷ and cloned in frame into the *NheI* site within the HA-tag coding region in the pcDNA3.1-HA-FOXO3 described by Asselin-Labat et al.³⁸ (with the mCherry insertion removing the HA-tag from the FOXO3 N-terminus). The following primer pair was used to amplify the mCherry coding sequence with *NheI* linkers:

mCherry_fwd:
TTAGCGCTAGCGCTGATATCGCTGCTGCTATGCTGAGCAAGGGCGAGG
mCherry_rev: TTAGCGCTAGCAGCCTTGTACAGCTCGTCCATGCCG

Realtime PCR. RNA from *Drosophila* larvae or adults was extracted with peqGOLD TriFast (peqlab)/chloroform in a Precellys homogenisator (peqlab), following the TriFast protocol. Extracted RNA was diluted in DEPC-treated water. For quantitative real-time PCR, 500 ng of RNA were used for cDNA synthesis with a QuantiTect Reverse Transcription Kit (Qiagen). A -RT reaction (without reverse transcriptase) with Actin5C primers was performed to control presence of genomic DNA in the RNA sample. Quantitative real-time PCR was performed with a CFX96 (Bio-Rad). PCR reactions consisted of first-strand cDNA template and iQSYBR Green Supermix (Bio-Rad). Actin5C and rp49 were used for normalization. Primers were chosen with minimal self- and 3' complementarity and CG content between 40% and 60%, and primer efficiency was tested using a cDNA dilution series. The following primer sets were used:

actin_fwd: GATCTGGCTGGTCCGCGATT
actin_rev: GGCCATCTCCTGCTCAAAGTC
rp49_fwd: TCTACCAGCTTCAAGATGAC
rp49_rev: CGAGAGAACAACAAGGTGGA
4E-BP_fwd: GAAGATTGAGGACCAGGAACA
4E-BP_rev: CGAGAGAACAACAAGGTGGA
InR_fwd: CACCCCGCTTCTATACTCCA
InR_rev: GTTAGGATGGTGGCCCTGTTC
Src42A_fwd: CTATGCGTCAACCTCTGCAA
Src42A_rev: TGGGGTCCATTGTACAGAT
Src64B_fwd: GATGCTGTGCCGAGAAG
Src64B_rev: CGTGTGTGATGCGTGTGAG

Immunostainings. Fatbodies from *Drosophila* larvae were dissected in *Drosophila* Ringer solution and fixed for 30 minutes in 3.7% formaldehyde in PBT (Roth), washed with 0.5% PBT and blocked with 5% Goat Serum (Gibco). Primary antibodies were incubated over night at 4°C. Fluorescence-labeled secondary antibodies were incubated for 1 h at room temperature. Tissue was washed with 0.1% PBT before being incubated with DAPI and mounted in Mowiol. As primary antibodies, we used mouse- α -GFP (Sigma) and rabbit- α -dFOXO against C- and N-terminus²⁴. As secondary antibodies, we used Alexa488-coupled goat- α -mouse and Alexa546-coupled goat- α -rabbit. DAPI was used as a nuclear counterstain. Fatbodies were mounted in Mowiol and analyzed with a Zeiss LSM 710 confocal microscope. Pictures were analyzed with Zeiss LSM Image Browser to show fluorescence intensity and with ImageJ to calculate the corrected total cell fluorescence (CTCF) value³⁹ with the formula $\text{IntDen} - \text{Area} \times \text{Mean of background} = \text{CTCF}$. For a quantitative analysis of nuclear dFOXO signal, the CTCF formula was applied only to the fluorescence intensity in the nuclear region in the confocal sections.

Starvation and larval inhibitor feeding. Eggs were collected for 4 h on apple juice agar plates with fresh yeast paste (42 g diluted with 6.5 ml of PBS). For starvation experiments, larvae were raised on the plates for 48 h and transferred to a dish with PBS-soaked filter paper for 24 h. For experiments with the Src inhibitor SU6656, flies were raised on apple juice agar plates for 48 h and transferred to fresh apple agar plates with fresh yeast paste mixed with 200 μ l of a 0.5 or 1 mM solution of the Src inhibitor, diluted in water from a 100 mM stock solution in DMSO. As a vehicle (negative) control, we added an equal quantity of DMSO without the inhibitor.

Statistics. We used the InStat program from GraphPad Software for statistical analyses and used the tests which were recommended by the program according to data input. For single comparisons, we used an unpaired, two-tailed Student's t-test to determine the p-value. For multiple comparisons, we used one-way ANOVA with Tukey-Kramer post test if the Kolmogorov-Smirnov (KS) test suggested normal distribution of the data points, and Kruskal-Wallis test with Dunn post test if the data did not pass the KS test (applies only to figure 3B). We used 0.05 as α -value for all statistical analyses. All experiments were carried out with at least 3 biological replicates, real-time PCR experiments with at least 5 biological replicates and 2 technical replicates each.

- Hunter, T. Signaling - 2000 and beyond. *Cell* **100**, 113–127 (2000).
- Martin, G. S. The hunting of the Src. *Nat Rev Mol Cell Biol* **2**, 467–475 (2001).
- Bilodeau, N. et al. Insulin-dependent phosphorylation of DPP IV in liver. Evidence for a role of compartmentalized c-Src. *Febs J* **273**, 992–1003 (2006).

- Park, S., Mazina, O., Kitagawa, A., Wong, P. & Matsumura, F. TCDD causes suppression of growth and differentiation of MCF10A, human mammary epithelial cells by interfering with their insulin receptor signaling through c-Src kinase and ERK activation. *J Biochem Mol Toxicol* **18**, 322–331 (2004).
- Schliess, F., Reissmann, R., Reinehr, R., vom Dahl, S. & Haussinger, D. Involvement of integrins and Src in insulin signaling toward autophagic proteolysis in rat liver. *J Biol Chem* **279**, 21294–21301 (2004).
- Xi, G., Shen, X. & Clemmons, D. R. p66shc inhibits insulin-like growth factor-I signaling via direct binding to Src through its polyproline and Src homology 2 domains, resulting in impairment of Src kinase activation. *J Biol Chem* **285**, 6937–6951, doi:10.1074/jbc.M109.069872 (2010).
- Xi, G., Shen, X., Radhakrishnan, Y., Maile, L. & Clemmons, D. Hyperglycemia-induced p66shc inhibits insulin-like growth factor I-dependent cell survival via impairment of Src kinase-mediated phosphoinositide-3 kinase/AKT activation in vascular smooth muscle cells. *Endocrinology* **151**, 3611–3623, doi:10.1210/en.2010-0242 (2010).
- Arbet-Engels, C., Tartare-Deckert, S. & Eckhart, W. C-terminal Src kinase associates with ligand-stimulated insulin-like growth factor-I receptor. *J Biol Chem* **274**, 5422–5428 (1999).
- Boney, C. M., Sekimoto, H., Gruppuso, P. A. & Frackelton, A. R., Jr. Src family tyrosine kinases participate in insulin-like growth factor I mitogenic signaling in T3T3-L1 cells. *Cell Growth Differ* **12**, 379–386 (2001).
- Lieskovska, J., Ling, Y., Badley-Clarke, J. & Clemmons, D. R. The role of Src kinase in insulin-like growth factor-dependent mitogenic signaling in vascular smooth muscle cells. *J Biol Chem* **281**, 25041–25053, doi:10.1074/jbc.M602866200 (2006).
- Peterson, J. E. et al. Src phosphorylates the insulin-like growth factor type I receptor on the autophosphorylation sites. Requirement for transformation by src. *J Biol Chem* **271**, 31562–31571 (1996).
- Sekharam, M., Nasir, A., Kaiser, H. E. & Coppola, D. Insulin-like growth factor I receptor activates c-SRC and modifies transformation and motility of colon cancer in vitro. *Anticancer Res* **23**, 1517–1524 (2003).
- Sun, H. & Baserga, R. The role of insulin receptor substrate-1 in transformation by v-src. *J Cell Physiol* **215**, 725–732, doi:10.1002/jcp.21352 (2008).
- Sun, H. Z., Xu, L., Zhou, B., Zang, W. J. & Wu, S. F. Depletion of insulin receptor substrate 2 reverses oncogenic transformation induced by v-src. *Acta Pharmacol Sin* **32**, 611–618, doi:10.1038/aps.2011.18 (2011).
- Datta, K., Bellacosa, A., Chan, T. O. & Tsichlis, P. N. Akt is a direct target of the phosphatidylinositol 3-kinase. Activation by growth factors, v-src and v-Ha-ras, in Sf9 and mammalian cells. *J Biol Chem* **271**, 30835–30839 (1996).
- Feng, X. T. et al. Palmitate contributes to insulin resistance through downregulation of the Src-mediated phosphorylation of Akt in C2C12 myotubes. *Biosci Biotechnol Biochem* **76**, 1356–1361 (2012).
- Jiang, T. & Qiu, Y. Interaction between Src and a C-terminal proline-rich motif of Akt is required for Akt activation. *J Biol Chem* **278**, 15789–15793 (2003).
- Liu, A. X. et al. AKT2, a member of the protein kinase B family, is activated by growth factors, v-Ha-ras, and v-src through phosphatidylinositol 3-kinase in human ovarian epithelial cancer cells. *Cancer Res* **58**, 2973–2977 (1998).
- Vojtechova, M. et al. Regulation of mTORC1 signaling by Src kinase activity is Akt1-independent in RSV-transformed cells. *Neoplasia* **10**, 99–107 (2008).
- Giot, L. et al. A protein interaction map of *Drosophila melanogaster*. *Science* **302**, 1727–1736 (2003).
- Cai, D., Dhe-Paganon, S., Melendez, P. A., Lee, J. & Shoelson, S. E. Two new substrates in insulin signaling, IRS5/DOK4 and IRS6/DOK5. *J Biol Chem* **278**, 25323–25330 (2003).
- Jünger, M. A. et al. The *Drosophila* Forkhead transcription factor FOXO mediates the reduction in cell number associated with reduced insulin signaling. *J Biol* **2**, 20 (2003).
- Kramer, J. M., Davidge, J. T., Lockyer, J. M. & Staveley, B. E. Expression of *Drosophila* FOXO regulates growth and can phenocopy starvation. *BMC Dev Biol* **3**, 5 (2003).
- Puig, O., Marr, M. T., Ruhf, M. L. & Tjian, R. Control of cell number by *Drosophila* FOXO: downstream and feedback regulation of the insulin receptor pathway. *Genes Dev* **17**, 2006–2020 (2003).
- Britton, J. S., Lockwood, W. K., Li, L., Cohen, S. M. & Edgar, B. A. *Drosophila*'s insulin/PI3-kinase pathway coordinates cellular metabolism with nutritional conditions. *Dev Cell* **2**, 239–249 (2002).
- Hennig, K. M., Colombani, J. & Neufeld, T. P. TOR coordinates bulk and targeted endocytosis in the *Drosophila melanogaster* fat body to regulate cell growth. *J Cell Biol* **173**, 963–974, doi:10.1083/jcb.200511140 (2006).
- Hay, B. A., Wassarman, D. A. & Rubin, G. M. *Drosophila* homologs of baculovirus inhibitor of apoptosis proteins function to block cell death. *Cell* **83**, 1253–1262 (1995).
- Lu, X. & Li, Y. *Drosophila* Src42A is a negative regulator of RTK signaling. *Dev Biol* **208**, 233–243 (1999).
- Tateno, M., Nishida, Y. & Adachi-Yamada, T. Regulation of JNK by Src during *Drosophila* development. *Science* **287**, 324–327 (2000).
- Blake, R. A. et al. SU6656, a selective src family kinase inhibitor, used to probe growth factor signaling. *Mol Cell Biol* **20**, 9018–9027 (2000).
- Brunet, A. et al. Akt promotes cell survival by phosphorylating and inhibiting a Forkhead transcription factor. *Cell* **96**, 857–868 (1999).



32. Buch, S., Melcher, C., Bauer, M., Katzenberger, J. & Pankratz, M. J. Opposing effects of dietary protein and sugar regulate a transcriptional target of *Drosophila* insulin-like peptide signaling. *Cell Metab* **7**, 321–332 (2008).
33. Pedraza, L. G., Stewart, R. A., Li, D. M. & Xu, T. *Drosophila* Src-family kinases function with Csk to regulate cell proliferation and apoptosis. *Oncogene* **23**, 4754–4762, doi:10.1038/sj.onc.1207635 (2004).
34. Cooper, J. A., Simon, M. A. & Kussick, S. J. Signaling by ectopically expressed *Drosophila* Src64 requires the protein-tyrosine phosphatase corkscrew and the adapter downstream of receptor kinases. *Cell Growth Differ* **7**, 1435–1441 (1996).
35. Brogiolo, W. *et al.* An evolutionarily conserved function of the *Drosophila* insulin receptor and insulin-like peptides in growth control. *Curr Biol* **11**, 213–221 (2001).
36. Dodson, G. S., Guarnieri, D. J. & Simon, M. A. Src64 is required for ovarian ring canal morphogenesis during *Drosophila* oogenesis. *Development* **125**, 2883–2892 (1998).
37. Shaner, N. C. *et al.* Improved monomeric red, orange and yellow fluorescent proteins derived from *Discosoma* sp. red fluorescent protein. *Nat Biotechnol* **22**, 1567–1572, doi:10.1038/nbt1037 (2004).
38. Asselin-Labat, M. L. *et al.* GILZ, a new target for the transcription factor FoxO3, protects T lymphocytes from interleukin-2 withdrawal-induced apoptosis. *Blood* **104**, 215–223, doi:10.1182/blood-2003-12-4295 (2004).
39. Gavet, O. & Pines, J. Progressive activation of CyclinB1-Cdk1 coordinates entry to mitosis. *Dev Cell* **18**, 533–543, doi:10.1016/j.devcel.2010.02.013 (2010).

Acknowledgments

This work was supported by an ETH Research Grant (TH-17 07-1) to MHB. We would like to thank Ruedi Aebersold for support, Ernst Hafen, Ross Cagan, Tian Xu, Takashi Adachi-Yamada, Roger Tsien, and the Bloomington *Drosophila* Stock Center for fly lines and reagents, and Gaia Tavosanis for helpful discussions on the project.

Author contributions

M.A.J., M.J.P. and M.H. conceived and supervised the project and M.H.B., T.R.B. and M.A.J. performed the experimental work. M.A.J. and M.H.B. wrote the paper. All authors reviewed the manuscript.

Additional information

Supplementary information accompanies this paper at <http://www.nature.com/scientificreports>

Competing financial interests: The authors declare no competing financial interests.

How to cite this article: Bülow, M.H., Bülow, T.R., Hoch, M., Pankratz, M.J. & Jünger, M.A. Src tyrosine kinase signaling antagonizes nuclear localization of FOXO and inhibits its transcription factor activity. *Sci. Rep.* **4**, 4048; DOI:10.1038/srep04048 (2014).



This work is licensed under a Creative Commons Attribution-NonCommercial-NoDerivs 3.0 Unported license. To view a copy of this license, visit <http://creativecommons.org/licenses/by-nc-nd/3.0>



SUBJECT AREAS:
GENETIC INTERACTION
CELL GROWTH
CANCER GENETICS
CANCER MODELS

CORRIGENDUM: Src tyrosine kinase signaling antagonizes nuclear localization of FOXO and inhibits its transcription factor activity

Margret H. Bülow, Torsten R. Bülow, Michael Hoch, Michael J. Pankratz & Martin A. Jünger

The labels of the x-axis of Figure 3A, B, and C are omitted in this Article. The correct Figure 3 appears below as Figure 1.

SCIENTIFIC REPORTS:
4 : 4048
DOI: 10.1038/srep04048
(2014)

Published:
11 February 2014
Updated:
7 July 2014

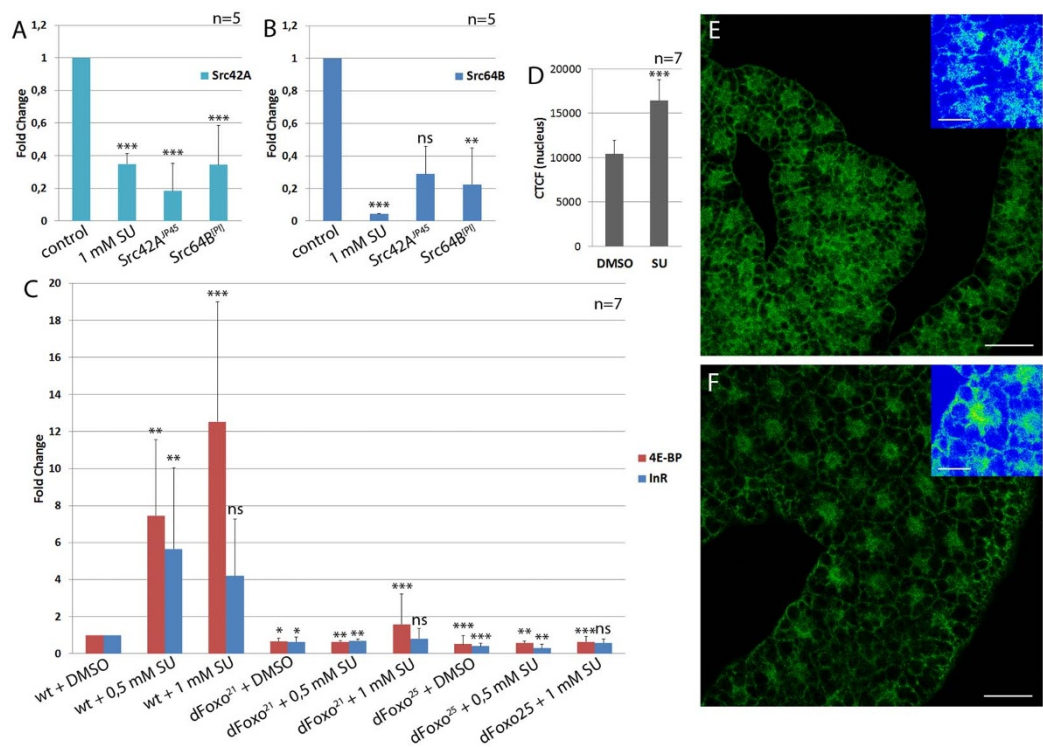


Figure 1 |